The effect of strain rate sensitivity on the prediction of the formability of advanced high strength steels

Marilena C. Butuc[1,2], *Toni* Chezan[3], and *Gabriela* Vincze[1,2,*]

[1]Centre of Mechanical Technology and Automation (TEMA), Department of Mechanical Engineering, University of Aveiro, 3810-193 Aveiro, Portugal
[2]LASI - Intelligent Systems Associate Laboratory, Guimarães, Portugal
[3]Tata Steel, P.O. Box 10.000, CA IJmuiden, 1970, Netherlands

Abstract. This paper analyzes the effect of strain rate sensitivity on the prediction of formability of advanced high-strength steels (AHSS). Three conventional dual-phase (DP) steels, 590DP, 980DP and 1180DP, and two third-generation AHSS grades with ultimate tensile strengths of 980 MPa and 1180 MPa are selected as reference materials. The onset of localized necking is simulated using the Marciniak-Kuczynski model, with the Yld2000-2d yield criterion defining the initial yield locus. The Swift strain-hardening power law, with and without strain rate sensitivity, is used to describe the material hardening behavior. A comparative analysis is carried out to assess the accuracy of forming limit predictions, with a particular focus on the influence of strain rate sensitivity. The results show that the Yld2000-2d yield criterion, combined with the Swift hardening law incorporating strain rate sensitivity, achieves the best agreement with experimental data. This study highlights the necessity of accounting for strain rate sensitivity in the Marciniak-Kuczynski model to improve the accuracy of forming limit predictions for advanced high-strength steels.

Keywords: Forming limits; Strain rate sensitivity; Marciniak-Kuczynski model; Advanced high strength steel.

1 Introduction

Advanced high-strength steels (AHSS) are crucial in modern manufacturing and automotive industries due to their exceptional strength-to-weight ratio, enabling lightweight structures, improved fuel efficiency, and enhanced crash safety without compromising performance. One major challenge facing both the steel and automotive industries is the failure of advanced high-strength steels, which impacts manufacturing efficiency, structural integrity, and overall performance. The Forming Limit Diagram (FLD) [1] is the most used method in the industry for assessing the sheet metal formability. Factors such as strain hardening, plastic anisotropy, strain rate sensitivity, and strain path influence forming limits. Theoretical analysis of plastic instability helps prevent failures, assess parameter effects on necking, and improve press performance. The Marciniak-Kuczynski (MK) model [2] is the main tool for predicting FLDs for various materials and deformation processes.

Stamping velocity is a key factor for economic efficiency of the manufacturing process [3]. While strain rate dependence is often ignored in simulations, some steels show significant strain rate sensitivity (SRS). This raises the question of whether considering strain rate sensitivity in flow behaviour can improve the accuracy of numerical simulations at lower stamping velocities, not just in high-speed applications. Vallaster et al. [4] explored the impact of strain rate-dependent material modelling on simulation accuracy in sheet metal forming processes using the steel HC340LA. Their material card improved forming force accuracy in deep drawing but significantly increased computation time. Larour et al. [5] found that bainite and martensite in a ferritic matrix reduce the strain rate sensitivity of automotive sheet steels, which further declines with increasing plastic strain due to work-hardening exhaustion and adiabatic softening. The m-value, expressing SRS, decreases with higher strength levels, particularly in mild, high-strength and high-strength low-alloy steels. Strain rate sensitivity stabilizes from above 0.05 in mild steels to around 0.01 in AHSS and ultra-high-strength steels. Xu et al. [6] used the MK and Bressan-William-Hill (BWH) [7] models with the Yld2000-2d yield function and Swift hardening law to predict the FLC of AISI409L and AISI430 stainless steels. The BWH model accurately matched

* Corresponding author: gvincze@ua.pt

experiments, while the MK model failed, regardless of SRS. They found that SRS had minimal effect on limit strains but influenced failure modes, with surface localized necking occurring in uniaxial and plane strain tension, and through-thickness shearing in balanced biaxial tension. Gutierrez et al. [8] found that the MK model accurately predicted FLCs in biaxial stretching but underestimated limit strains in uniaxial stretching for three AHSS. To improve FLD predictions for third-generation AHSS with ultimate tensile strengths (UTS) of 980 MPa and 1180 MPa, they proposed modifications to the Bressan-Williams model and the modified maximum force criterion MMFC [9]. Butuc et al. [10] found that the strain rate sensitivity of USS CR980XG3™ AHSS, a third generation of AHSS has a significant impact on the prediction of forming limit strains through the MK model.

The purpose of this paper is to investigate the influence of the strain rate sensitivity on the prediction of forming limits for a wide range of advanced high strength steels using the MK model. The constitutive equations applied in the MK model are the Yld2000-2d yield function and the Swift hardening law with and without SRS. The study examines three conventional dual-phase steels, 590DP, 980DP, and 1180DP, along with two third-generation AHSS grades with UTS of 980 MPa (acronym 3gen980) and 1180 MPa (acronym 3gen1180). Material model parameters were determined based on experimental data from literature. A comparative analysis of experimental and predicted forming limits is carried out to evaluate the accuracy of the predictions, emphasising the effect of strain rate sensitivity.

2 Theoretical forming limit strain calculation

2.1 Marciniack-Kuczynski analysis

The simulation of plastic instability is conducted within the framework of heterogeneous materials using the Marciniak-Kuczinski analysis in conjunction with the Theory of Plasticity. The MK model focuses on the growth of an initial defect, represented by a narrow band inclined at an angle ψ_0 relative to the principal axis. The initial value of the geometrical defect (f_0) is characterized by the ratio of the initial thicknesses in the homogeneous region and the groove. The theoretical computation of the MK model is described in [11]. The stress and strain states are calculated using the selected constitutive equations. Plastic flow localization occurs when the effective strain increment in the band is 10 times greater than in the homogeneous region. The forming strain limits are defined by the principal strains in the homogeneous region at the onset of necking, and the FLD limit point for each strain path is determined by minimizing these principal strains relative to ψ_0. The analysis assumes rigid plasticity behaviour, plane stress conditions, and isotropic work hardening of the material.

The numerical results of the present study were simulated using FLDcode [11], a modular, user-friendly software designed to predict plastic flow localization under both linear and complex strain paths.

2.2 Hardening model

The Swift hardening law (acronym Swift) expresses the strain hardening as a power law:

$$\sigma = K(\varepsilon_0 + \bar{\varepsilon})^n \quad (1)$$

where σ is the flow stress, $\bar{\varepsilon}$, the effective plastic strain, K, the strength coefficient, ε_0, the reference strain and n, the strain hardening coefficient.

A modified version of Swift that takes the strain rate sensitivity (acronym Swift_m) into account is:

$$\sigma = K(\varepsilon_0 + \bar{\varepsilon})^n \dot{\bar{\varepsilon}}^m \quad (2)$$

where $\dot{\bar{\varepsilon}}$ is the strain-rate and m the strain rate sensitivity coefficient.

2.3 Yield criteria

The Yld2000-2d plane stress yield function of Barlat et al. [12] (acronym YLD00-2d) introduces plastic anisotropy by using two linear transformations on the Cauchy stress tensor. It is expressed in terms of the deviatoric stress components as:

$$\phi = \phi'(\tilde{\mathbf{S}}') + \phi''(\tilde{\mathbf{S}}'') = 2\overline{\sigma}_Y^a \quad (3)$$

where $\overline{\sigma}_Y$ is the effective stress, a is an exponent connected to the crystal structure, and, ϕ' and ϕ'' are two isotropic functions defined by

$$\phi'(\tilde{\mathbf{S}}') = \left|\tilde{S}'_1 - \tilde{S}'_2\right|^a \quad (4)$$

$$\phi''(\tilde{\mathbf{S}}'') = \left|2\tilde{S}''_2 + \tilde{S}''_1\right|^a + \left|2\tilde{S}''_1 + \tilde{S}''_2\right|^a \quad (5)$$

$\tilde{\mathbf{S}}'$ and $\tilde{\mathbf{S}}''$ are the linear transformations of the effective stress tensor $\boldsymbol{s}$ defined as the deviatoric part $\boldsymbol{\sigma}'$ of the Cauchy stress:

$$\tilde{\mathbf{S}}' = \mathbf{C}'\mathbf{s} \quad , \quad \tilde{\mathbf{S}}'' = \mathbf{C}''\mathbf{s} \quad (6)$$

where $\mathbf{C}$' and $\mathbf{C}$'' contain the material anisotropy coefficients.

3 Results and discussion

3.1 Materials

The studied materials include DP590, DP980, DP1180, 3Gen980, and 3Gen1180, with experimental data sourced from [13] and DP590* from [14]. Their parameters are summarized in Table 1.

Table 1. Materials parameters from [13] and *[14]

	DP 590	DP 590*	DP 980	DP 1180	3gen 980	3gen 1180
σ_0/σ_0	1	1	1	1	1	1
σ_{45}/σ_0	0.995	0.997	0.988	1.004	0.971	1.001
σ_{90}/σ_0	1.019	0.976	1.018	1.025	0.998	1.022
σ_b/σ_0	1	1.03	1	1	1	1
R_0	0.67	0.91	0.78	0.82	0.86	0.76
R_{45}	1.08	0.85	1.03	0.95	0.93	0.93
R_{90}	0.9	1.12	0.95	0.98	0.9	0.9
R_b	1	0.884	0.84	0.94	1	0.92

The Swift parameters are given in Table 2. They were identified from the experimental data of Noder et al. [13], except for those of DP590*, which were sourced from [14].

Table 2. Swift parameters.

	DP 590	DP 590*	DP 980	DP 1180	3gen 980	3gen 1180
K	1050	942.9	1400	1908	1650	1680
ε_0	0.005	0.0035	0.0003	0.005	0.001	0.00142
n	0.16	0.15	0.08	0.13	0.18	0.087
m	0.01	0.01	0.01	0.01	0.01	0.0099

The anisotropy parameters for the Yld2000-2d yield function are presented in Tables 3 and 4. They were numerically identified using experimental data: r_0, r_{45}, r_{90}, r_b, σ_0, σ_{45}, σ_{90}, σ_b, from Table 1. The exponent "a" of Yld2000-2d is typically 6 for materials with a Body-Centred Cubic (BCC) crystal structure and 8 for those with a Face-Centred Cubic (FCC) structure. However, alternative values are used, especially for new structural materials [8, 10, 20]. Various values of the exponent "a" were applied in the identification of the yield function coefficients to evaluate how the sharpness of the yield locus under equibiaxial stretching influences the predicted forming limits.

Table 3. Anisotropy coefficients of the Yld2000-2d yield function for DP steels.

	DP590		DP590*	DP980	DP1180
a	6	8	6	6	6
α_1	0.889	0.937	0.909	0.973	0.975
α_2	1.037	0.995	1.101	0.981	0.982
α_3	1.059	0.969	0.909	0.988	1.037
α_4	0.995	0.982	0.985	0.986	0.988
α_5	1.014	0.998	1.002	1.017	1.007
α_6	0.916	0.893	0.938	1.003	0.970
α_7	1.011	1.005	0.977	1.012	0.991
α_8	0.996	1.038	1.079	1.023	1.000

Table 4. Anisotropy coefficients of the Yld2000-2d yield function for 3gen AHSS.

	3gen980	3gen1180		
a	6	6	8	10
α_1	0.969	0.965	0.987	0.996
α_2	1.005	0.977	0.966	0.962
α_3	0.993	1.017	1.013	1.014
α_4	1.006	0.991	0.991	0.99
α_5	1.007	1.013	1.009	1.007
α_6	0.979	0.972	0.985	0.989
α_7	1.015	0.991	0.993	0.995
α_8	1.086	1.011	1.007	1.005

3.2 Forming Limit Diagrams

In this study, the experimental forming limit diagrams from Noder et al [13] were used for all selected materials. In addition, for DP590* steel, supplementary experimental results from various sources [15-17] have been considered. The strain paths are defined by the stress ratio (α), expressed as σ_2/σ_1, and the strain ratio (ρ), expressed as $d\varepsilon_2/d\varepsilon_1$. The acronyms UT, PS, and BS refer to uniaxial tension, plane strain, and biaxial stretching, respectively. The FLD's left side corresponds to the region between UT and PS, while the right side represents the area between PS and BS. The experimental forming limits under proportional loading, and those simulated using the Yld2000-2d yield function and Swift hardening law (with and without strain rate sensitivity), are presented in Fig. 1 for DP590, Fig. 2 for DP590*, Fig. 3 for DP980, Fig. 4 for 3Gen980, Fig. 5 for DP1180, and Fig. 6 for 3Gen1180. Several values for the initial value of the MK geometrical defect were chosen, adjusting the imperfection factor for each material until the best fit with the experimental data is achieved. Specifically, the value of f_0 was set to 0.9993 for the Swift hardening law across all materials, except for DP590* (f_0=0.9998) and DP1180 (f_0=0.991). For Swift_m, various f_0 values were applied: 0.998 for DP590*, 0.997 for DP590, 0.996 for DP980 and 3Gen1180, 0.992 for 3Gen980, and 0.989 for DP1180. In the case of Swift hardening law, the right side of the FLD is overestimated for all materials, except DP1180, while the left side of the FLD is underestimated for DP590, DP590*, DP980 and 3gen1180. Taking into account the strain rate sensitivity in simulation and adjusting MK geometrical value increases the accuracy of the predicted results. This effect, observed in most of the selected materials, is explained using DP590 steel with a=8 as an example. As shown in Fig. 1, incorporating strain rate sensitivity (m=0.01) in the modified Swift equation, shifts the FLD upwards, increasing the forming limits across the entire range. Conversely, applying a geometrical defect value of 0.997 shifts the FLD downwards, reducing the forming strain limits, with a more pronounced effect in the stretching zone. This adjustment improved the predicted shape of the FLD, leading to better reproducibility of the experimental data.

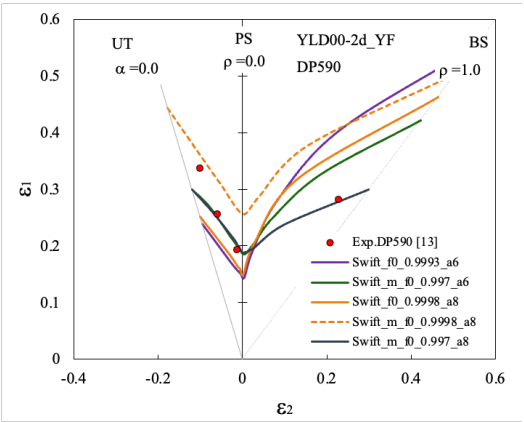

Fig. 1. Experimental and theoretical FLDs for DP590 using Yld2000-2d yield function with Swift and Swift_m hardening laws, at various f_0 values.

As observed in Fig. 1, for DP590 steel, Yld2000-2d with Swift_m allows accurate FLD prediction when using an exponent "a" of 8, a value that aligns with the findings of Lou et al. [20]. The forming limits predicted with a=6, even when considering SRS, are overestimated on the right side of the FLD.

For DP590* steel, the experimental forming limits from various references, presented in Fig. 2, show the greatest discrepancy in the plane strain region, emphasising the need for reliable experimental data. The predicted FLD using Swift follows the same trend as the previously studied DP590. The inclusion of strain rate sensitivity improves the accuracy of the predicted forming limits within the experimental range.

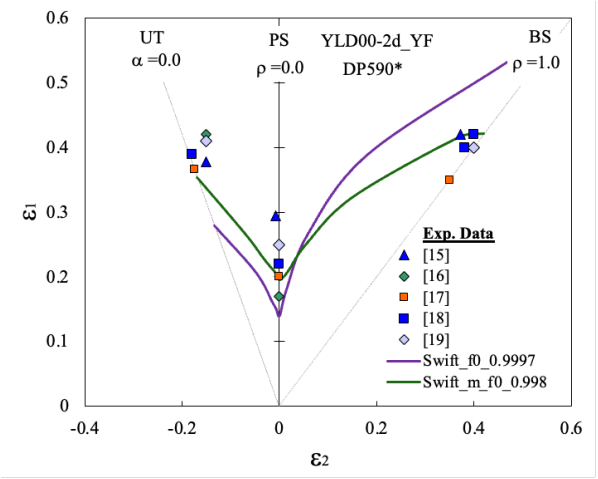

Fig. 2. The effect of SRS (m) and f_0 value on the prediction of FLDs for DP590* steel.

The same trend is observed for DP980 steel in Fig. 3 and 3Gen980 steel in Fig. 4, highlighting the significant impact of strain rate sensitivity on the accuracy of the predicted FLD. A good correlation between experimental and theoretical forming limits calculated using Swift_m is achieved for DP980 steel with an f_0 of 0.996, and even more remarkable for 3Gen980 steel with an f_0 of 0.992.

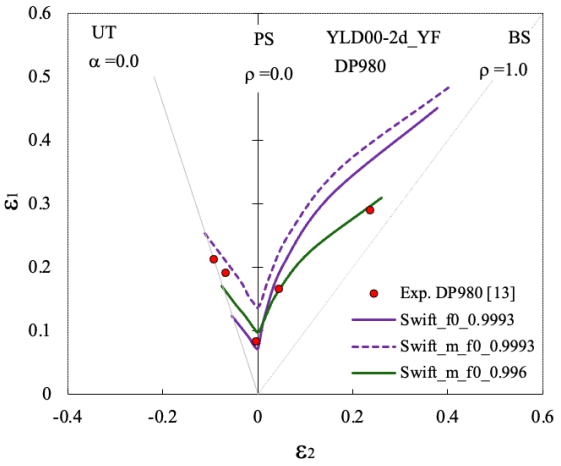

Fig. 3. The effect of SRS (m) and f_0 value on the prediction of FLDs for DP980 steel.

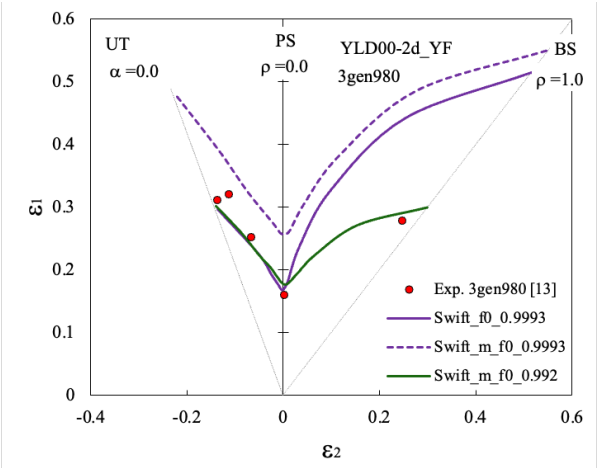

Fig. 4. The effect of SRS (m) and f_0 value on the prediction of FLDs of 3gen980 steel.

Butcher et al. [21] found that the MMFC model provided a more accurate FLD prediction for DP1180 steel compared to the MK model. Fig. 5 shows that for DP1180, the predicted FLD without SRS shows good agreement with the experimental data, except in uniaxial tension where it is underestimated. When the strain rate sensitivity is taken into account, the predicted forming limits are overestimated in the plane strain region, while they are in good agreement with the experimental forming limits in uniaxial tension and biaxial extension.

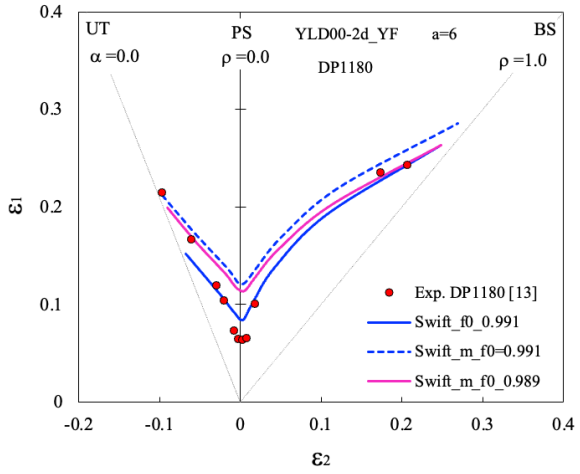

Fig. 5. The effect of SRS (m) and f_0 value on the prediction of FLDs of DP1180 steel.

Fig. 6 presents experimental forming limits for 3gen1180 steel [13] obtained using various methods: Marciniak tests with non-linear strain path (NLSP) correction (Exp.Marciniak-NLSP), Nakazima tests with NLSP correction (Exp.Nakazima-NLSP), and Nakazima tests with both NLSP and contact pressure correction (Exp.Nakazima-NLSP+P).

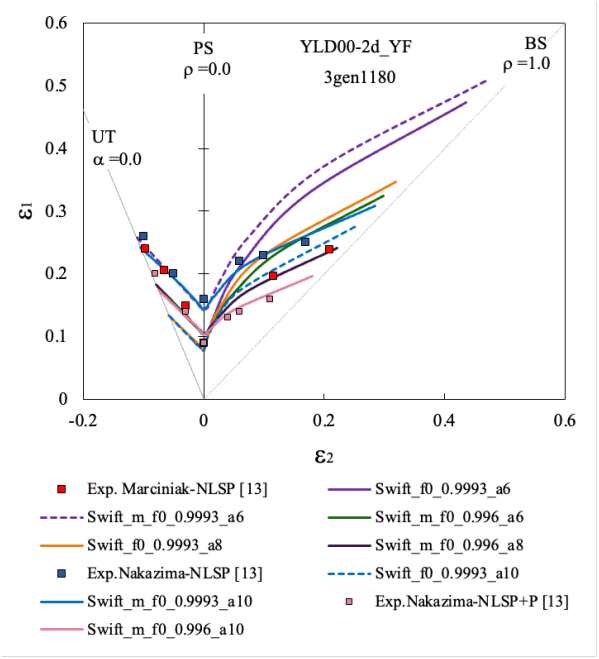

Fig. 6. Experimental and theoretical FLDs of 3gen1180 steel showing the effect of f_0, m and a.

When compared with all these experimental cases, the predicted FLD obtained with YLD00-2d with an exponent "a" of 6, without SRS, is underestimated on the left side and overestimated on the right side, accurately reproducing only the experimental forming limit in the plane strain region. Applying values of "a" of 8 and 10, respectively, in the Yld00-2d yield function, improves the accuracy on the right side of the FLD, without any effect on the left side. The predicted FLD with SRS and using "a" of 10, accurately reproduces the Exp.Nakazima-NLSP data with f0 of 0.9993 and the Exp.Nakazima-NLSP+P, with f0 of 0.996, while using a of 8 reproduces the Exp.Marciniak-NLSP. Improvements in the predicted forming limits are also found for "a" of 6 with SRS and f0 of 0.996. These results demonstrate the flexibility of the MK model in simulating various experimental datasets obtained through different methods, highlighting the need for accurate and consistent experimental measurements.

4 Conclusions

The onset of localized necking for various AHSS has been simulated using a sheet metal forming limit model based on the Marciniak-Kuczynski analysis combined with the Yld2000-2d yield function and the Swift hardening law, with and without SRS. A sensitivity study of the effect of the strain rate sensitivity, on the forming limits has been performed. Incorporating strain rate sensitivity in the Marciniak-Kuczynski model improves the accuracy of forming limit predictions for most advanced high-strength steels.

Acknowledgments

The authors acknowledge support from the Portuguese Foundation of Science and Technology (FCT), in its State Budget component (OE) through project (https://doi.org/10.54499/2022.05783.PTDC) 2022.05783.PTDC. This article was also supported by the UID Centro de Tecnologia Mecânica e Automação (TEMA).

References

1. M. Gensamer M., Trans ASM **36**:30, (1946).
2. Z. Marciniak and K. Kuczynski, K., Int. J. Mech. Sci. **9**, 609, (1967).
3. R. Neugebauer, K-D, Bouzakis, B. Denkena, F. Klocke, A. Sterzing, E.A. Tekkaya, R. Wertheim, CIRP Ann, **60**:627, (2011)
4. E. Vallaster, S. Wiesenmayer, M. Merklein, Prod. Eng. **18** (1):47, (2024)
5. P. Larour, A. Bäumer, K. Dahmen, W. Bleck, Steel Res. Int. **84**:426, (2013)
6. L. Xu, F. Barlat, D.C. Ahn, J.D. Bressan, Sci Eng A **528** (7-8):3113 (2011).
7. J. D. Bressan, J. A. Williams, Int J Mech Sci **5**:155 (1983).
8. J. E. Gutierrez, J. Noder and C. Butcher, Metals **10**, 902, (2020)
9. P. Hora, L. Tong, B. Berisha, Int J Mater Form **6**, 267, (2013).
10. M. C. Butuc, G. Vincze, R. Santos, A. Pereira, A. D. Santos, R. L. Amaral, F. Barlat, Int. J. of Mech. Sci. **281**, 109559, (2024).
11. M. C. Butuc, C. Teodosiu, A. Barata da Rocha, J.J. Gracio, Eur. J. Mech. A Solids **30**, 532, (2011).
12. F. Barlat, J. C. Brem, J. W. Yoon, K. Chung, R.E. Dick, D.J. Lege, F. Pourboghrat, S.-H. Choi, E. Chu, Int J Plast **19**, 1297, (2003).
13. J. Noder, J. E. Gutierrez, A. Zhumagulov, J. Dykeman, H. Ezzat and C. Butcher, Materials **14**, 4970, (2021).
14. J.-W. Lee, M.-G. Lee, F. Barlat, Int. J. Plast **29**, 13 (2012).
15. Z. G. Ma, Z. Liu, X. Jiang, K. Wu, M. Diao, M. Wan, Mat. and Design **96**, 401, (2016)
16. J. Samei, D. E. Green, J. Cheng, M. S. C. Lima, Mat. and Design **92**:1028, (2016)
17. S. Basak, S. K. Panda, J. Mater. Process. Technol. **267**, 289, (2019)
18. K.-H. Chung, W. Lee, J. H. Kim, C. Kim, S.H. Park, D. Kwon, K. Chung, Int. J. Solids Struct. **46**, 344, (2009).
19. H. Park, S.-J. Kim, J. Lee, D. Kim, *Determination of forming limits of high strength sound-deadening laminated sheet*, IOP Conf. Series: J. phys: Conf. Series **1063,** 012015, (2018).
20. Y. Lou, S. Kim, C. Lee, H. Huh, *Prediction of forming limit diagrams of DP590 steel based on the M-K model with experimental verification*, in Proceedings of the 10th Asia-Pacific Conference, AEPA, 100104, 61, 15-17 November 2010, Wuhan, China (2010).

21. C. Butcher, F. Khameneh, A. Abedini, D. Connolly, S. Kurukuri, J. Mater. Process. Technol. **287**: 116887 (2021).